CFD ANALYSIS OF MICROCHANNEL HEAT SINK COOLING SYSTEM FOR HIGH CONCENTRATION PHOTOVOLTAIC SYSTEMS

Jorge Andrés Arroyave Ortegón

João Pedro Cassiano

jaaoinc@gmail.com

jpedrocassiano@gmail.com

Elaine Maria Cardoso

João Batista Campos Silva

emcfisica@gmail.com

jbcampos.silva@gmail.com

UNESP – São Paulo State University

Av. Brasil, n°56, Centro, 15385-000, Ilha Solteira, São Paulo, Brazil.

Abstract. *Solar energy could be used as a thermal energy source using solar collectors or as an electric energy source using photovoltaic cell systems. However, photovoltaic cells have some limitations regard higher temperatures and non-homogeneous temperature distributions carrying these systems to shortening its useful life and also decreasing its electrical efficiency, all this added to the costs of the photovoltaic cell materials. These limitations have been the focus of researchers in this field trying to improve the electrical efficiencies, operation temperatures and reducing the materials needed. Thus, this work aims to analyze the performance of a heat sink based on parallel microchannels for cooling a HCPV (high concentration photovoltaic) cell through a theoretical, numerical (using commercial CFD software Ansys FLUENT V15) and experimental analysis. In this work, it was considered the worst case scenario (no electricity generation), the maximum radiation peak and the average radiation according to the weather reports obtained by the UNESP - CANAL CLIMA located at São Paulo State northwest region. The focus of the model is thermal analysis, so optical efficiency on concentrators and electrical analyses are defined as input data. It is found that the use of microchannel heat sinks can improve the efficiency of a HCPV cell by introducing an effective thermal management. The temperature rise across the microchannel is estimated as10K for a commercial HCPV cell with an effective area of 100 mm^2, and the pressure drop is estimated as 940 Pa for a mass flux of 330 kg/m^{2}s.*

Keywords: *Solar energy, HCPV systems, Microchannel heat sink.*

1 INTRODUCTION

Solar energy can be used mainly in two ways: the first one is taking advantage of the thermal potential of solar radiation and the second one, is using the photovoltaic effect generating electricity.

Solar thermal potential is harnessed with the help of solar collectors, which are a group of irradiated surfaces that receives solar radiation converting it into heat that is transferred to a working fluid. Afterwards, the working fluid can be used in applications such as water and environment heating (domestic applications), electric co-generation or water desalinization (industrial applications). Solar collectors have some constraints related to heat absorption capabilities due to the physical properties on the irradiated surface materials (absorber) and the low thermal conductivity of working fluids.

Eshghi et al. (2013) present the option of replace these solid absorbers (superficial process) for liquid absorbers (volumetric process) reducing the thermal resistances and therefore increasing efficiency. Javadi et al. (2012) show some advances associated with addition of nanoparticles in a base fluid (nanofluids) in solar collectors, finding conductivity improvements around 20 - 40% just by adding 1% in volume of these particles. However, these techniques and surrounding phenomena are not completely understood and require more studies in depth.

Electricity generation is the other alternative for solar energy use; it is generated with photosensitive materials producing electric current that could be used as a power source for different applications. These sensitive materials forms a photovoltaic cell, which in turn, can form a photovoltaic generation system, however depending on the type of system, these cells do not necessarily constitute the most important part of such systems.

Photovoltaic generation systems may vary according to their application, simplest systems are built with flat plate solar panels, the PV cells in these panels are formed generally of silicon, and systems that are more complex may include thermal generation or solar radiation concentrators adding equally relevant components. Such relevant components can be concentrations optics (if the system is a concentration system), a solar tracker, an electric inverter or a cooling system (Petito et al., 2013).

The usage of these elements depends on system application. The reason for that is based on the new technologies proposals for solar generation: Concentrating PV systems (CPV) and High Concentration Photovoltaic systems (HCPV), where optical elements are used to concentrate in one point solar radiation, increasing the amount of energy available, and thus reducing the necessary photosensitive material, *i.e.*, the PV cell will have less area (Kleinstreuer et al., 2014).

Nevertheless, despite of the benefits of PV systems use, we find limitations in its efficiency and reliability since not all the solar energy can be converted into electricity and cells materials have restrictions with high operation temperatures, *i.e.*, electrical conversion efficiency depends on surface temperature and its distribution on it (Carriere et al., 2015). These limitations have been overcome with the introduction of multi-junction solar cells as an alternative to single layer silicon cells. This kind of cells uses materials from groups III-V on periodic table, and the temperature tolerance according to manufacturers may be around 180 °C and electrical efficiencies above 40%.

Nonetheless, this is not enough to face the high temperatures issues, especially in CPV and HCPV systems. Therefore, cooling systems were introduced allowing researchers to focus their works on new proposals in this area trying to balance its consumptions (pumping and solar trackers systems power in active cooling systems) or making too complex designs (passive cooling systems). Dey et al. (2005) present the bases and principles of cooling systems in solar concentration systems: cell temperature control, simple design and low power consumption. They reported that impingement jets and microchannel heat sinks are the most adequate cooling systems to work with HCPV systems.

Microchannel heat sink is based on use of multiple ducts allowing to a working fluid (water or refrigerant) dissipate heat through it. The definition of microchannel comes from the values of hydraulic diameter and, we can consider as a microchannel all the ducts with diameters lower than 3 mm (Do Nascimento, 2012).

Pease and Tuckerman (1981) developed a new concept based on compact heat sink devices for very large-scale integrated circuits cooling. The authors showed the limitations on systems using air as working fluid (passive cooling) and how simple concepts like thermal resistance plays an important role on its design and performance.

These developments gives to solar energy systems notable improvements related to their limitations in terms of high temperatures, low electrical conversion efficiency and, how reducing the investments needed to implement these systems as a real alternative to traditional energy sources based in fossil fuels.

In this way, works are focused in develop theoretical models estimating parameters like PV cells operating temperatures and power generated, as the studies proposed by Almonacid et al. (2014a,b). The authors compared several methods for performance assessing, by using meteorological values (ambient temperature, wind speed, direct radiation), indirect methods, and direct methods based on measurements on heat sink (temperatures on the heat sink, electricity generated). Other researchers focus on working fluids with the use of nanofluids (solution with nanoparticles addition on a base fluid) and the development of appropriate models in CPV applications (Kleinstruer et al., 2014).

Yang et al. (2015) present CPV systems using microchannel cooling technique. Temperature differences around 6 °C through microchannel inlet and outlet plus pumping power lower than 5% of net power are some remarkable results with these kinds of systems. Also, Escher et al. (2010) prove the influence of thermal resistance in PV cell-heat sink interface showing us how reducing the materials layers on it with a silicon plate as heat sink.

Other works present analysis related to the heat transfer process by studying the boiling phenomena behavior (liquid-vapor) in microchannel heat sinks. One of these studies was performed by Halemic (2011), where he found how the vapor quality could influence the performance of this process and how the special characteristics of the boiling process could enhance the heat flux dissipated.

At this point, it is clear how solar electric generation works towards more efficient and reliable devices pushing solar energy as a real solution. The present work takes advantage of Brazil solar energy generation potential with at least 25% of his territory been irradiated with values above 1800 kW-h/m^2/year according to Martins et al. (2011), and particularly in the southwest region where is located the Sao Paulo State.

Thus, the present reasearch aims to develop a theoretical, numerical and experimental analysis of a microchannel heat sink in a HCPV system. The first two analyses are the bases for the experimental development. The study presented here includes an evaluation of these systems according to the weather conditions at São Paulo State northwest region, and also, theoretical comparisons with simplest designs.

2 METHODOLOGICAL PROCEDURES

The research project is divided in three stages: i) theoretical analysis, ii) numerical analysis and iii) experimental analysis. As already mentioned, this article presents partial results for stages i) and ii).

It is necessary to define input values that depend on PV cells characteristics, weather conditions and cooling system operation, such as: PV cells manufacturer information (dimensions, efficiency, temperature influence, etc.); weather records at São Paulo State northwest region (wind speed, solar radiation rates, temperature, etc.); and, material physical properties as well as literature correlations.

Manufacturer information is summarized in Table 1. It was chosen some models of HCPV cells comparing them with three parameters: effective area or useful irradiated area on cell surface, electrical efficiencies as the measure of PV cell solar radiation conversion and maximum temperature for PV cell.

Table 1. HCPV cells manufacturer information.

	Effective area [mm^2]	Efficiency [%]	$T_{max.}$[°C]
Azurspace HCPV cell model: 3C44A	100	42.1	110
Spectrolab HCPV cell model: CCA 100 C1MJ	97.42	37	100
Spectrolab HCPV cell model: C4MJ	86.47	40	110
Spectrolab HCPV cell model: C3P5	30.71	39.5	110
Azurspace HCPV cell model: 3C42A	100	41.2	110

The HPCV cell choose was model 3C42A manufactured by Azurspace with a maximum efficiency of 41.2% (considering standard conditions at AMD 1.5 and surface temperature of 25 °C), and an effective area of 100 mm^2.

Weather data strongly influences the efficiency of the HCPV system. Table 2 shows a set of weather database obtained by using the UNESP - CANAL CLIMA historic records for São Paulo State northwest region for one-year interval (jan – dec 2016). For this period, we have mean and maximum values: the first ones were taken in the whole year period, and the second ones were taken from the month with highest peak of radiation (jan 2016). For HCPV systems those values correspond to mean and maximum operation points, respectively.

Table 2. Mean and maximum weather database values.

	Period	Direct radiation [MJ/m^2]	Mean temperature [°C]	Wind speed [m/s]	Insolation [h/day]
Mean. values	Jan-Dec 2016	9.85	24.6	1.6	6.45
Max. values	Jan-2016	18.8	35.7	2.7	7.5

The another group of input variables and parameters will be defined from materials physical properties as thermal conductivity, density, viscosity and others associated with co-relations from the literature (Kleinstruer et al., 2014).

It is important to define the geometry for our case study. This geometry is based on Do Nascimento (2012) by using a microchannel based heat sink design with rectangular and constant cross-section. The heat sinks with this kind of characteristics are common due to its benefits such as a simple design, which helps with manufacturability issues due to small dimensions. The heat sink proposed considers the selected HCPV cell effective area, 10 mm *x* 10 mm. The copper microchannel heat sink consists of 33 parallel rectangular channels of 10 mm in length, 200 µm in width and 0.5 mm in height for each microchannel, as presented in Figure 1.

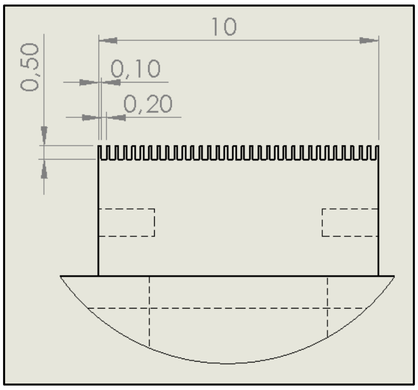

(a)

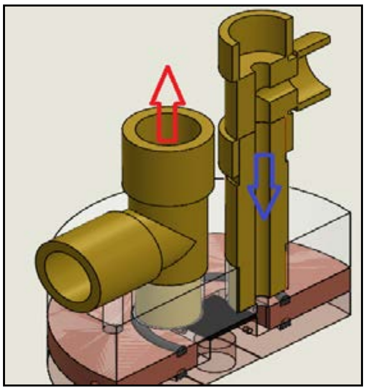

(b)

Figure 1. Microchannel heat sink. (a) microchannel detail section; (b) working fluid path.

2.1 Theoretical methodology procedure

Theoretical model involves a system of equations based on energy balance whose solution give us values for the heat dissipated, radiation losses, convection losses and cell temperature as a function of the flow conditions.

Model focus is thermal analysis, so optical (optical efficiency on concentrators) and electrical (inverter and pump efficiencies) analyses are defined as an ideal case with 100% efficiency (no losses).

Heat sink energy balance is presented in Eq. (1):

$$0 = i_{solar} + w_{electric} + q_{conv} - q_{rad} - q_{cond} \tag{1}$$

where:

i_{solar}: $concentrated\ radiation\ flux\ through\ cell\ surface$

$w_{eléctric}$: $electric\ generation\ power$

q_{conv}: $convection\ loss$

q_{rad}: $radiation\ loss$

q_{cond}: $heat\ flux\ to\ be\ dissipated\ from\ the\ cell\ through\ conduction$

Radiation flux should be defined according to Table 2 (direct radiation and insolation) multiplying it by the optics geometrical ratio (500*x*) which will give us the value for i_{solar} on Eq. (1). Electric generation is function of cell efficiency and, i_{solar}.

Convection and radiation losses can be calculated by using the flat plate approximation on the cover and the Stefan-Boltzmann law, respectively. For q_{cond}, we use the thermal resistance method for cell temperature calculation:

$$R_{equi.} = \frac{T_{cell} - T_{wall}}{q_{cond} * A} \tag{2}$$

Thermal resistance is calculated from materials properties and *A* is the cell effective area. T_{cell} depends on T_{wall}, and the wall temperature depends on flow conditions. This can be solved by using the Newton's law of cooling (Eq. 3), and the constant heat flux through an internal wall case (Eq. 4). It is important to say that $q''_{conv} = q''_{cond}$ because the heat transferred to the heat sink through conduction is the same heat to be transferred to our working fluid with the convection mechanism.

$$q''_{conv} = h_x(T_{wall} - T_m) \tag{3}$$

$$T_m(x) = T_{m,i} + \frac{q''_{cond}P}{\dot{m}c_p}x \tag{4}$$

where h_x is defined as the local heat transfer coefficient; $T_m, T_m(x)$ and $T_{m,i}$ the mean, the local and the inlet temperature for working fluid, respectively. P the cross-section perimeter; $\dot{m}$ the working fluid flow rate and, finally, c_p the specific heat for our working fluid.

We use the methodology proposed by Lee and Qu (2007), where this type of problems are analyzed including the approach by fins for microchannels. In this method, the authors define three types of parameters: Geometric parameters (heat sink and microchannel dimensions), operating parameters (conditions in which the heat sink must operate) and thermal/fluid parameters.

Using those parameters defined in our previous step with the set of equations proposed by Lee and Qu (2007), it is possible to determine T_{wall} if we know $\dot{m}$, then we suppose a flow rate and iterates until T_{cell} falls in the desirable value defined by cell efficiency. The set of equations allows calculate the temperatures and also the heat transfer coefficient and pressure drop, ΔP. Finally, the thermal resistance method is coupled with the methodology proposed by Lee and Qu (2007), and T_{cell} is found with Eq. (2).

The theoretical approach have some considerations such as, steady state flow, one-dimension problem, uncompressible flow, constant heat flux through the heat sink surface, and Reynolds number up to 2300 (according to the methodology reviewed). This approach, allow us to check the heat sink response to the worst case condition, *i.e.*, 100% heat dissipation and not electrical generation.

2.2 Numerical methodological procedure

Numerical analysis is based on CFD software Ansys FLUENT V15. The governing equations will be the Navier-Stokes equations, considering uncompressible flow (water is used as working fluid).

Pre-analysis and geometry selection. This analysis considers a tridimensional geometry, it is applied for the entire microchannels and, the inlet and outlet plenums are also considered. Then, from Fig. 1b (fluid path) we have three circular pieces - two in copper and the other one in polycarbonate - that forms our numerical problem geometry.

The problem will be coupled considering the conduction problem through the copper pieces and the convection problem (the working fluid dissipating heat from microchannel surface), assuming a constant heat flux over the solar cell effective area. However, we are going to restrict the numerical analysis to the convection problem getting the hydrodynamic solution with the velocity field distribution and also temperature profiles through this geometry.

Figure 2 shows the flow domain for our numerical problem geometry. The heat flux q will be distributed through microchannel sides with one exception, the top side where the polycarbonate piece will isolate the heat sink. The inlet and outlet regions are going to be treated as isolated as well. Input data will be used with some theoretical analysis results trying to understand the qualitative behavior of our problem.

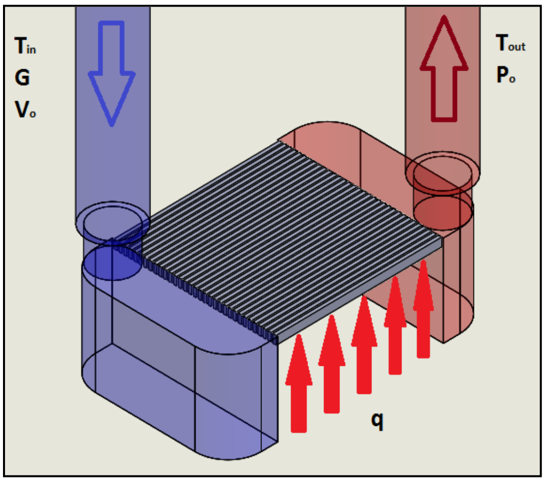

Figure 2. Numerical problem geometry.

Mesh generation. We divided our geometry in three regions to obtain a refined mesh in the microchannels and to better analyze the geometrical differences on fluid domain.

Figure 3a shows regions 1 and 2 as the inlet and outlet ducts. At these regions our mesh will use the hexahedral dominant method trying to keep some homogeneity in the global mesh. Figure 3b shows region 3, the microchannels region, where we use 100% hexahedral elements defining longitudinal and transversal divisions, trying to keep some proportionality in them due to the differences between both dimensions.

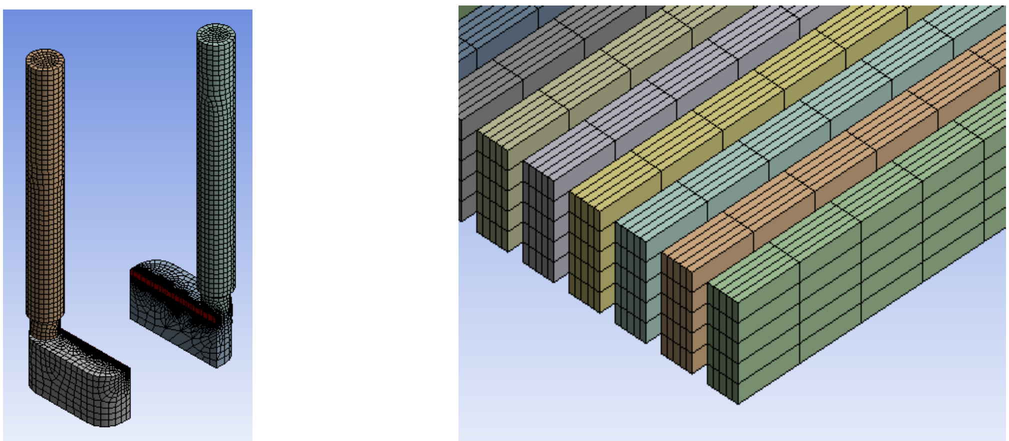

(a) (b)

Figure 3. Mesh generated. (a) Inlet and outlet regions and (b) Microchannel region.

Solution method. The SIMPLE scheme is our best option due to the lesser computational time required compared with another schemes like the coupled one. SIMPLE scheme precision is acceptable for our analysis purpose after testing and comparing both schemes.

The spatial discretization was defined with second order upwind schemes for pressure, momentum and energy. Gradient discretization used the least squares cell based method due to the benefits in computational time required.

Figure 4a presents the boundary conditions. Inlet velocity was calculated with a mass balance between microchannel inlet flow rate (*G* value from theoretical approach) and the geometry inlet (B tag in the Fig. 4a). Atmospheric pressure was defined as a pressure reference, and therefore, outlet pressure was set up as zero taking in account the characteristics of our problem (low-pressure system). No slip condition is applied on all surfaces (red surfaces in Fig. 4a).

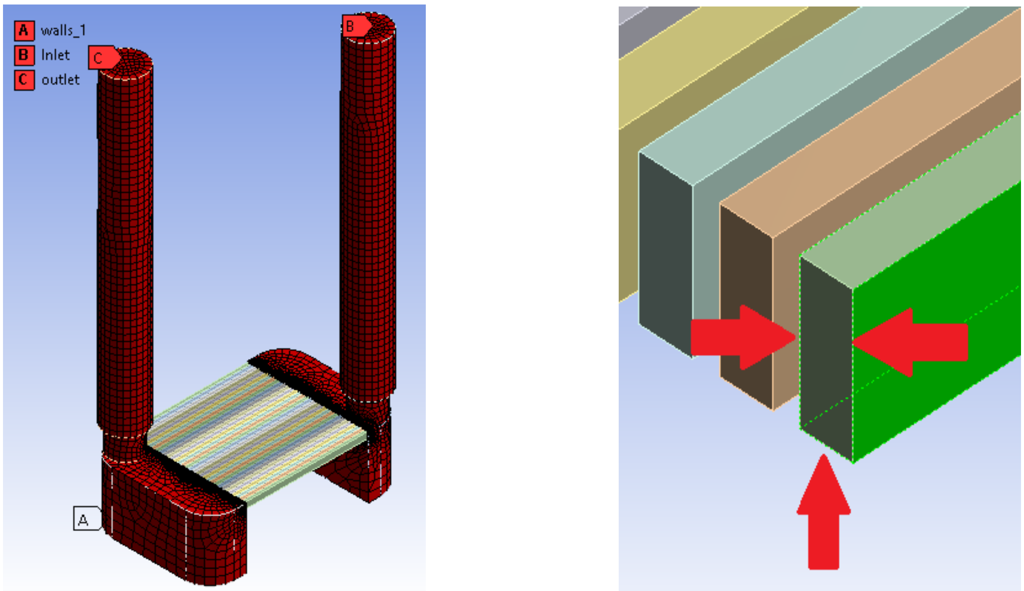

(a) (b)

Figure 4. Boundary conditions definition. (a) Inlet and outlet regions and (b) microchannel region.

Temperature conditions, *i.e.*, energy equation boundary conditions, are presented in Fig. 4b. The walls were considered isolated (adiabatic walls) except the microchannel region, which has three surfaces (base and sides) with constant heat flux applied, and the missing surface isolated (top). For inlet and outlet boundary conditions, the temperature was 25 °C and 40 °C, respectively, due to theoretical analysis results.

Convergence criterion by residual monitors was defined as absolute, using tolerance values for continuity equation below of 10^{-4}, meanwhile for momentum equations below 10^{-6}.

Verification and validation. Verification step is based on theoretical results considering the following parameters:

- Convergence achieved
- Pressure, temperature and velocity contours in defined regions
- Pressure drop through defined microchannel
- Velocity variation through defined microchannel
- Temperature variation through defined microchannel

Input values are the same for theoretical and numerical approaches and, if numerical solution is consistent its solution should be qualitatively and quantitative closer to theoretical solution. Thus, we compared both analysis results by using velocity variation through microchannel, pressure drop and temperatures distribution. Likewise, qualitatively we expect to have fully developed flow through microchannel, higher pressure at the microchannel inlets compared with the microchannel outlet (normal response on laminar and fully developed flows).

Validation of these results will be performed with the experimental results; however, this corresponds to the next step for this project.

3 RESULTS AND DISCUSSIONS

3.1 Theoretical analyses

Using the input data mentioned in the previous section, the values for electric power, natural convection losses at the surface, radiation and dissipative heat conduction were obtained, as shown in Table 3. The cell was analyzed with a geometrical concentration ratio of 500*x* and with an electrical efficiency of 40%. Two situations were considered:

• (A) Thermal analysis made for mean values obtained from UNESP - CANAL CLIMA with cell operating in ideal conditions.

• (B) Thermal analysis made for the maximum values obtained from UNESP - CANAL CLIMA with cell operating in ideal conditions.

Table 3.Values of solar incidence, electric power, air convection, radiation and conduction for situations (A) and (B).

Flux analysis	Mean (A)	Maximum (B)
Solar incidence 500*x* [kW/m^2]	212.10	348.15
Electric power [kW/m^2]	82.10	134.77
Air convection [kW/m^2]	0.12	0.05
Radiation [kW/m^2]	0.08	0.25
Conduction [kW/m^2]	129.79	213.08

Comparing convection and radiation losses, with solar incidence or electrical power, the influence of them is negligible for both cases. It is important consider the differences regard to solar incidence in case A and B (around 64% higher), showing that the analysis should focus on the case when the cell is not generating electricity (*i.e*., all the radiation should be dissipated by the cooling system).

Table 4 shows the results for the worst scenario, which means that the database considers the data from case B assuming no electricity generation. Here we have three important results to remark: firstly, the total mass flow rate will benefit the pressure drop in microchannels ensuring lower power consumptions. Secondly, cell surface temperature keeps around 45 °C leading to a potential electrical efficiency around 39%. Finally, the inlet and outlet temperature difference for the working fluid and wall is lower than 10 °C, which leads to temperature variations homogeneous in the cell surface.

A comparison with a single rectangular heat sink was also carried out, assuming the same global dimensions, 10 mm *x* 10 mm *x* 0.5 mm, and the same considerations. Figure 5 and 6 show these results, varying only the mass velocity value, G [kg/m^{2}s].

Table 4. Theoretical analysis results.

	Worst scenario (100% dissipation)
Heat Flux [kW/m^2]	348
Mass velocity [kg/m^{2}s]	330
Flow rate [ml/min]	65.56
Inlet temp. [°C]	25.0
Outlet temp. [°C]	33.9
Base inlet temp. [°C]	33.9
Base outlet temp. [°C]	42.7
Cell surface mean temp. [°C]	45.9
Pressure drop [Pa]	1116.40
Reynolds number	122.68

Figure 5 presents the results for cell temperature for heat sink based on parallel microchannels and for heat sink based on single rectangular channel. From the results, one may observe the performance vantages for microchannels over single channel heat sink design - microchannels introduce an effective thermal management.

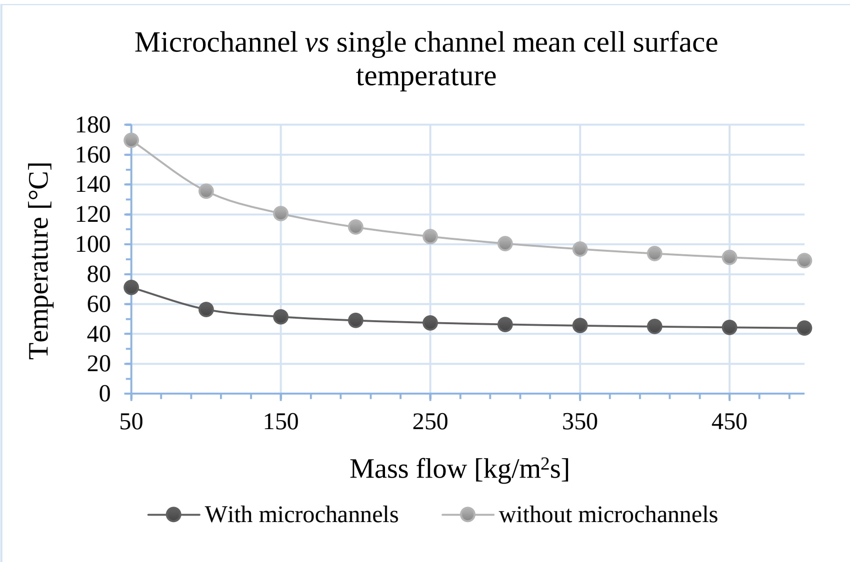

Figure 5. Cell surface temperature *vs* mass velocity for different heat sinks design.

In addition, these results present an asymptotic temperature behavior, where higher flows do not represent higher temperature reductions (increasing G value from 50 to 100 kg/m^{2}s gives a temperature reduction of 20%; however, from 450 to 500 the reduction is only 1%). This behavior indicates an optimum mass velocity value around 500 kg/m^{2}s for our heat sink design when the temperature trend to keep stable around 40 °C.

Pressure drop behavior is shown in Fig. 6. It is possible to observe a clear trend of growth for microchannel heat sinks; however, the values are acceptable when compared to the benefit provided by these systems, *e.g.*, at the operation point considered (G = 330 kg/m^{2}s) the pressure drop for the microchannel heat sink is 18 times greater, but since the cell efficiency is 8% higher and the lifetime is also increased due to the lesser operation temperature, the use of these cooling systems are justified.

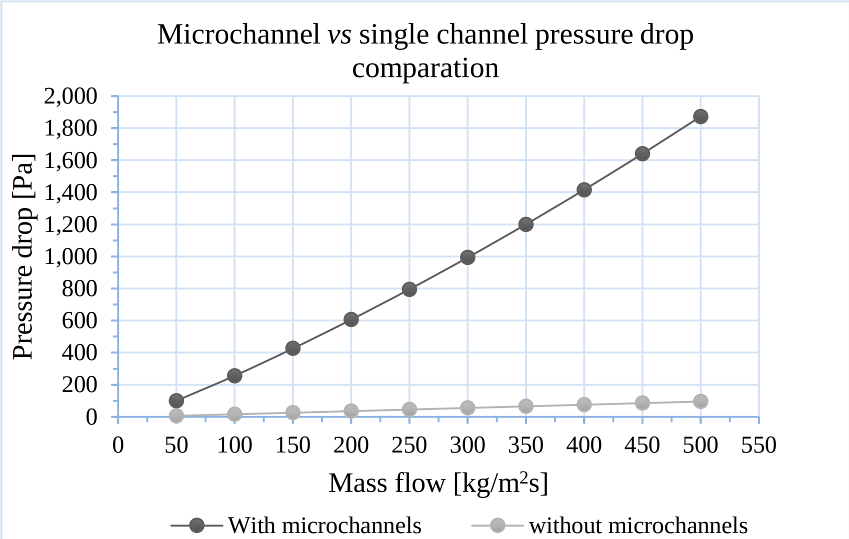

Figure 6. Pressure drop *vs* mass velocity for different heat sinks design.

Both results show microchannel heat sink vantages but also presents clearly limitations regard the minimum temperature on the heat sink and also how important is it to propose designs considering thermal improvements but also considering pressure drop on them.

3.2 Numerical results and discussion

Numerical results focused on the worst case (100% heat dissipation) because the performance of the heat sink will be validated for the entire operating range of the solar cell.

Figure 7 presents the temperature contours through microchannel walls, showing how wall temperature increases as a natural response to the decrease in the temperature gradient between working fluid and wall temperatures. Despite of the contours present a homogeneous distribution, we found temperature differences through microchannel inlet and outlet around 15 °C. In addition, the temperature values through microchannel outlet points present a suddenly reduction (around 5 °C). This behavior may be due to the change in the geometry when it passes from microchannel shape to ducts shape, increasing the local heat transfer coefficient.

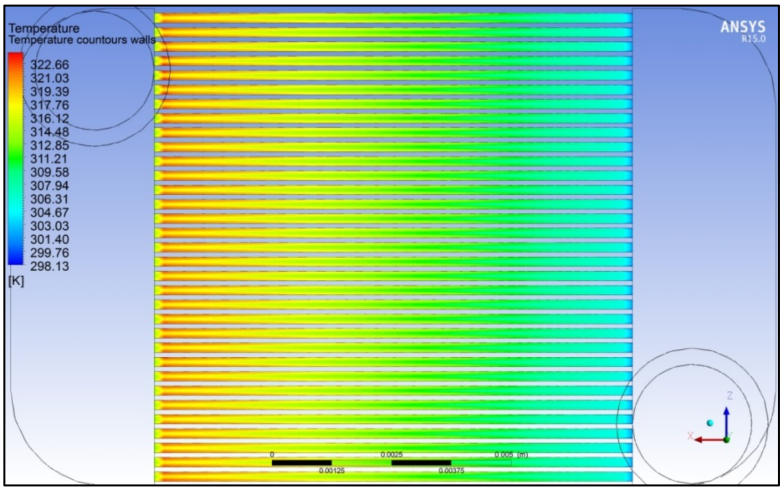

Figure 7. Temperature contours through microchannel walls (inlet duct at the right side).

Figure 8 shows the working fluid temperatures contours. There is a lower temperature difference between inlet and outlet (compared to the walls) around 5 °C. In addition, it is important to see how the mixing effect is present on fluid as it increases its temperature around walls while it is flowing through microchannels.

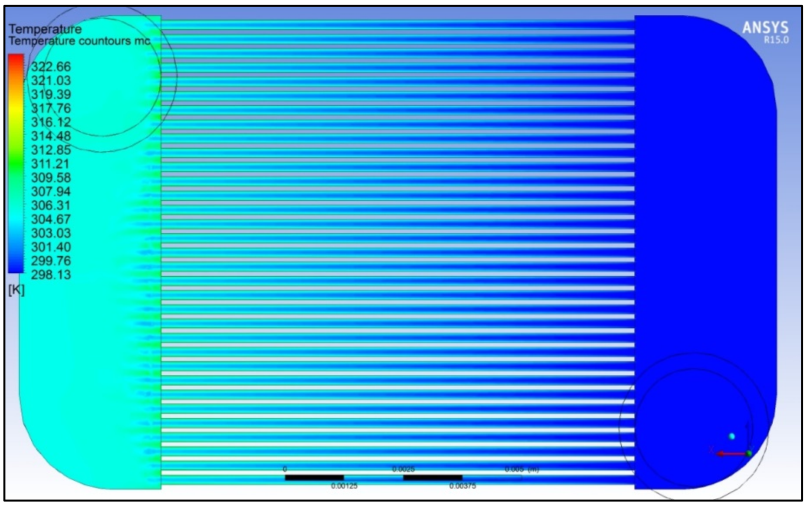

Figure 8. Working fluid temperature contours (inlet duct at the right side).

Velocity countors, Fig. 9, allow us to see how the flow is becoming fully developed in all microchannels keeping little variations at inlet but particularlly showing a chimeney effect at the outlet, reducing the velocity when the fluid arrives to the outlet point.

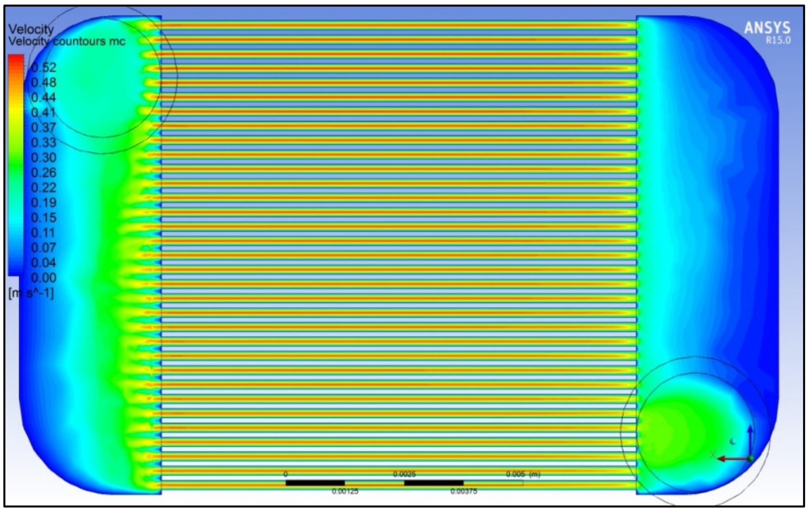

Figure 9. Velocity contours (inlet duct at the right side).

Temperature and velocity, Figures 7 and 9, have a particular response at the outlet, coupling their effects and improving the heat transfer process in the wall.

Figure 10 presents wall and fluid temperature variations. Reviewing the results presented on Table 4, we found out that for the working fluid the outlet temperature is a little lower, reducing the temperature difference, being 8.3 °C on theoretical results and 5 °C for numerical results. Also for wall temperatures we found theoretical values of 42.7 °C and numerical values of 40 °C influenced for the reducing effect on the outlet.

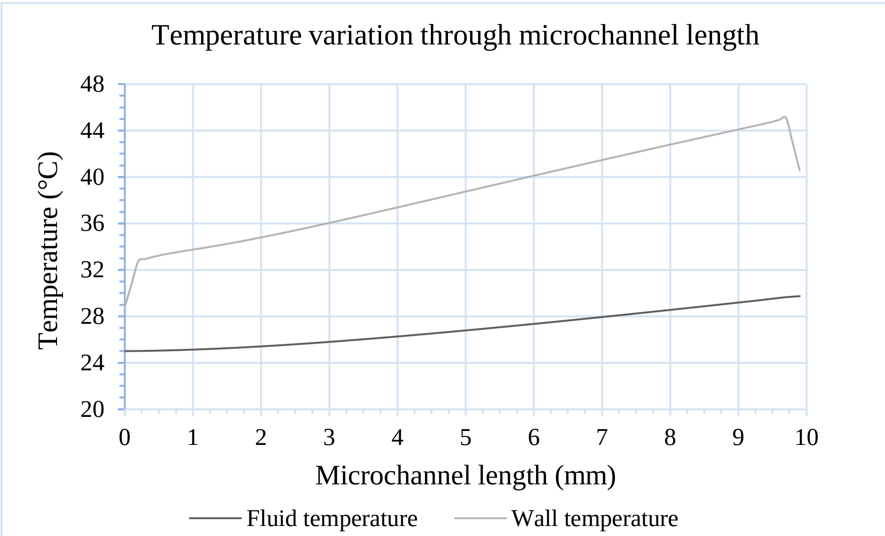

Figure 10. Wall and fluid temperature variations through mid-section microchannel.

Velocity variations, Fig. 11, show the fully developed behavior with an entrance region where velocity is increasing achieving a constant value around 0.5 m/s and the length entrance is approximately 1.50 mm. Comparing these results with the theoretical ones, we found

Proceedings of the XXXVIII Iberian Latin-American Congress on Computational Methods in Engineering
P.O. Faria, R.H. Lopez, L.F.F. Miguel, W.J.S. Gomes, M. Noronha (Editores), ABMEC, Florianópolis, SC, Brazil, November 5-8, 2017.

consistency due to the same magnitude order between both results, *i.e.*, the theoretical entrance length is 1.62 mm and the inlet velocity is around 0.34 m/s.

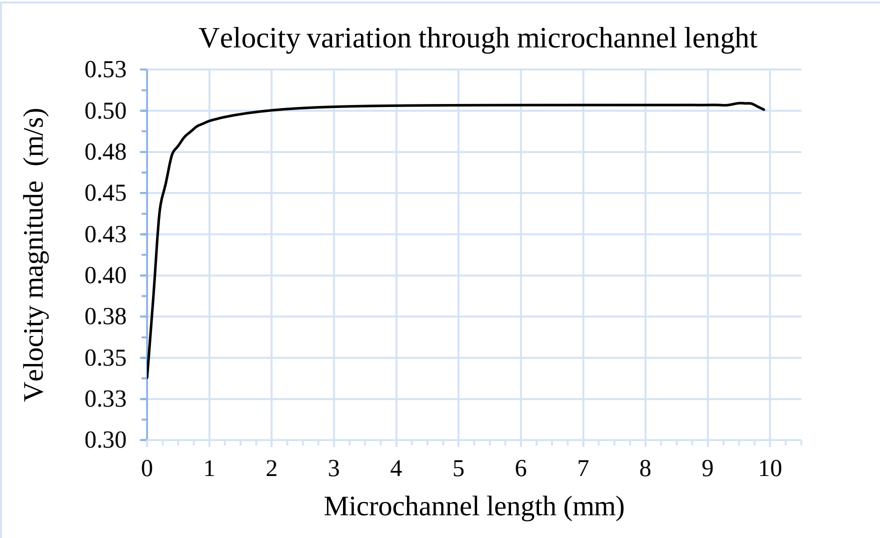

Figure 11. Velocity variations through mid-section microchannel.

The microchannel pressure drop for the theoretical approach is 1116.4 Pa, meanwhile in our numerical analyses is 940 Pa. This is expected since the theoretical analysis considered a one-dimensional case instead of the tri-dimensional analysis performed in the numerical case.

Our verification step for numerical analyses close with a mass flux residuals equal to $3.85x10^{-7}$ and with a heat rate dissipated of 34.8 W (according to effective area) which are acceptable for our problem.

4 CONCLUSIONS

Theoretical and numerical results indicate that the proposed heat sink based on parallel microchannels is capable to dissipate a heat flux of 348 kW/m^2 in an effective area of 10 mm *x* 10 mm, keeping the heat sink surface at a mean temperature 40 °C with a low pressure drop, 940 Pa. Also, comparing the microchannel heat sink with a single rectangular channel heat sink the temperature differences at the same conditions compensate the higher pressure drops of the first, for mass velocity values in the range of 400 - 500 kg/m^{2}s.

The analyses performed in the present study give an appropriate view on microchannel performance compared to the macrochannel for single-phase problems (small differences are expected due to the assumptions made it for each approach). The present results will be compared with experimental data in order to validate the numerical approach. Thus, the next step will be the experimental validation taking as a base the results presented and, also, to develop a deeper analysis regards the proposed design vantages and disadvantages for future works.

ACKNOWLEDGEMENTS

The authors are grateful for the financial support from the PPGEM – UNESP/FEIS, from the National Counsel of Technological and Scientific Development of Brazil (grant number 458702/2014-5) and from FAPESP (grants numbers 2013/15431-7 and 2016/20481-1).

REFERENCES

Almonacid, F., Fernández, E.F., Pérez-Higueras, P., Rodrigo, P., 2014a. A method for estimating cell temperature at the maximum power point of a HCPV module under actual operating conditions, *Solar energy materials & solar cells*, vol. 124, pp. 159–165.

Almonacid, F., Fernández, E.F., Pérez-Higueras, P., Rodrigo, P., 2014b. Calculation of the cell temperature of a high concentrator photovoltaic (HCPV) module: A study and comparison of different methods, *Solar energy materials & solar cells* vol. 121, pp. 144–151.

Carriere, C., Dollet, A., Elouamari, R., Levrier, B., Salins, J.E. de, Sicre, M., Tsanakas, J.A., Vossier, A., 2015. A novel approach of accelerated ageing tests for high concentration III–V multijunction solar cells through rapid irradiation/thermal cycles, *Solar Energy*, vol. 116, pp. 205–214.

Dey, C.J., Mills, D.R., Royne, A., 2005. Cooling of photovoltaic cells under concentrated illumination: a critical review, *Solar Energy Materials & Solar Cells*, vol. 86, pp. 451–483.

Do Nascimento, F.J., (2012). *Estudo teórico-experimental da transferência de calor e da perda de pressão em um dissipador de calor baseado em microcanais*. M.Sc. Thesis, University of São Paulo.

Escher, W., Ghannam, R., Khalil, A., Michel, B., Paredes, S., 2010. Advanced Liquid Cooling for concentrated Photovoltaic electro-thermal co-generation presented in: *Thermal issues in emerging technologies*, Cairo Egypt.

Eshghi, A.T., Kasaeian, A., Sameti, M., 2013. A review on the applications of nanofluids in

School of mechanical and system engineering University of Newcastle.

Javadi, F.S., Saidur, R., Kamalisarvestani, M., 2012. Investigating performance improvement of solar collectors by using nanofluids, *Renewable and Sustainable Energy Reviews*, vol. 28, pp. 232-245.

Kleinstreuer, C., Xu, Z., 2014. Concentration photovoltaic–thermal energy co-generation system using nanofluids for cooling and heating, *Energy conversion and management*, vol. 87, pp.504-512.

Lee, S., Qu, W., 2007. Thermal design methodology for low flow rate single-phase and two-phase micro-channel heat sinks, *IEEE transactions on components and packaging technologies*, vol. 30, no. 4.

Martins, F.R., Pereira, E.B., Rüther, R., Viana, T.S., 2011. Assessing the potential of concentrating solar photovoltaic generation in Brazil with satellite-derived direct normal irradiation, *Solar Energy* vol. 85, pp. 486–495.

Pease, R.F.W., Tuckerman, B.D, 1981. High-Performance heat sinking for VLSI, *IEEE eléctron device letters*, vol 2.

Petito, F., Renno, C., 2013. Design and modeling of a concentrating photovoltaic thermal (CPV/T) system for a domestic application, *Energy and buildings.* vol. 62, pp. 392-402.

Yang, k., Zuo, C., 2015. A novel multi-layer manifold microchannel cooling system for concentrating photovoltaic cells. *Energy conversion and management*, vol. 89, pp. 214-221.